2023 IEEE/ASME International Conference on Advanced Intelligent Mechatronics (AIM)
June 28-30, 2023. Seattle, Washington, USA

Musculoskeletal Model Construction of Deep Squat Using Low-Cost Inertial Measurement Units

Guohui Wang, Yu Chen, Minda Wang, Yifan Wang*

***Abstract*—Squatting is a compound exercise that can provide strong stimulation to the entire lower limb and trunk, positively affecting cardiovascular functions, neural regulations, and hormone secretion. In addition, squatting is commonly involved in labor intensive tasks where potential injuries may happen, and assistive devices are needed. In this study, we developed a low-cost IMU data acquisition system for capturing human squatting movements, with a total cost of only ~500 UGD. We conducted experiments on normal squats and knee valgus squats. The data obtained is imported into the OpenSim software for analysis, and we obtain experimental results on joint angles, joint moments, muscle forces, and metabolism. The results show that incorrect squatting postures can increase the burden on the hip joint. Additionally, during the squatting process, the tibialis anterior muscle had the highest activation level, while the soleus muscle had the greatest force. Our experimental and simulation results provide guidelines for future design and optimization of exoskeletons to assist humans during squat motions while reducing the risk of injuries.**

***Keywords*—Squat, OpenSim, IMU, Exoskeletons.**

I. INTRODUCTION

Squatting is a compound exercise that involves bending the hips and knees to push the body towards the ground and then returning to a standing position. Squats stimulate the entire lower limb and trunk, and can exercise the quadriceps, glutes, hamstrings, and other muscles. Squatting has a positive effect on a series of physiological and biochemical responses, such as cardiovascular functions, neural regulations, and hormone secretion. Therefore, it has been widely used in clinical evaluations [1]–[4]. In addition, squatting is commonly involved in labor intensive tasks, such as workers lifting heavy weights from the ground, during which injuries may occur. Analyzing the musculoskeletal model during squat may help to provide guidelines on the future design of exoskeletons that can assist during squat movements.

In recent years, there has been increasing interest in the biomechanics of squats, together with the potential benefits and risks associated with this exercise. Many studies have used OpenSim software to investigate joint angles, muscle activation, and strength involved in squatting. Florian Schellenberg et al. [5] used OpenSim to simulate and analyze the knee flexion angle during the squatting process. Lu et al. [6] explored the effect of hindfoot eversion on squatting biomechanics. Li et al. [7] analyzed the different biomechanical loads that novice female practitioners exhibit during full and half squat exercises, providing reference for correcting squatting postures. C.A. Gallo et al. [8] and O. Bordron, C. et al. [9] simulated and analyzed the squatting motion using OpenSim software. Yichen Lu et al. [10] compared the lower limb loads during squatting between Asian and Caucasian populations using an OpenSim musculoskeletal model. These simulation analyses provide valuable information for exercise prescription and rehabilitation plans.

Currently, when using OpenSim for squat motion analysis, motion-tracking cameras are commonly used for data collection. However, it is difficult to record the squatting process in free living situations. Inertial Measurement Units (IMUs), which can estimate 3D sensors and segmented directions, have become an attractive alternative for 3D motion capture systems. Some scholars have studied the system combination of IMU data and OpenSim [11], [12]. However, most IMU-based motion capture systems use expensive and closed-source commercial sensor systems such as Xsens [13] or APDM[14], [15], which are difficult for ordinary users to afford [16], [17], and to integrate in affordable assistive devices. Therefore, referring to the solution proposed in [18], we have built a low-cost IMU data acquisition system and applied it to the squatting process. In situations where super high precision is not required, this system has the advantages of low cost, and the ability to collect data without being restricted by the user location or environment.

The contribution of this work includes several aspects:

(1) An IMU data acquisition system was developed for squat posture analysis, which can capture the lower limb status of the human body in real-time.
(2) Based on this system, data collection and simulation analysis of normal squatting and knee valgus squatting were conducted. Parameters including joint angles, moments, muscle forces, and metabolic conditions were then obtained. This provides a baseline and guide for the subsequent development of assistive exoskeletons for squats.

The structure of this article is as follows. Section II introduces the IMU motion-capture system and experimental settings. Section III analyzes the experimental results. Section IV discusses the experimental results and provides guidance for exoskeleton design. Finally, Section V summarizes our findings.

This research was supported by A*STAR Singapore through RIE2025 MTC IRG award (M21K2c0118) and RIE2020 AME YIRG award (A2084c0162), and the NAP award (020482) from Nanyang Technological University.

Corresponding author: Yifan Wang: yifan.wang@ntu.edu.sg

Guohui Wang, Yu Chen, Minda Wang, and Yifan Wang are with the School of Mechanical and Aerospace Engineering, Nanyang Technological University, Singapore 639798.

II. METHODS

A. Motion capture prototype

A healthy male participant, aged 24, with a weight of 58.8 kg and a height of 172.7 cm, was recruited for this study. He had no muscle or skeletal injuries or diseases. The participant provided informed consent to participate in the study. The experiments performed in Nanyang Technological University were approved by the ethics committee. The experimental procedures adhered to the *Helsinki Declaration*.

In reference to [18], a low-cost human motion capture system was assembled for this study. The system comprises eight 9-axis IMU sensors, a Raspberry Pi computer, Qwiic connector cables, and USB rechargeable batteries. The type and unit price of each component are shown in table 1. The total cost of the capture system is approximately 500 USD. Compared to commercial motion capture systems such as Xsens (approximately 40,000 USD), this system has a strong price advantage.

TABLE. I Low-cost human motion capture system components.

Component Name	***Model***	***Unit Price (USD)***	***Quantity***
Raspberry Pi	4B (4GB RAM)	269	1
IMU	Basic Starter Kit Adafruit LSM6DSOX + LIS3MDL - Precision 9 DoF IMU	22	8
Qwiic Connector Cables	SparkFun- PRT-14429	1.92	20
Qwiic Mux Breakout	SparkFun- BOB-16784	13.55	1
Strap	/	1.50	10
Rechargeable Battery	/	15.00	1

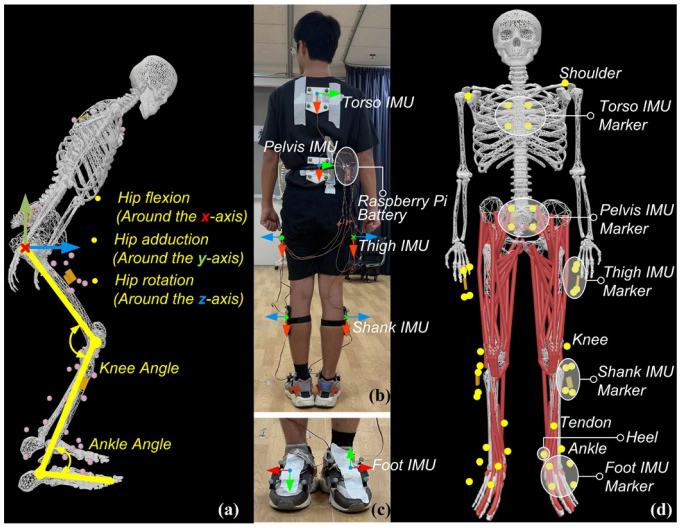

Fig.1 (a) Lower body joint movement angle during deep squat. (b) Components and orientation settings of low-cost IMU-Based human motion capture system. (c) Schematic illustration of the foot IMU orientation. (d) Schematic illustration of the optical acquisition system's marker setting

Fig. 1(a) depicts the angles at which the lower body joints move during a deep squat. Hip flexion, hip adduction, and hip rotation are the primary thigh movements in relation to the hip. The knee angle is the rotation of the shank in relation to the thigh. Ankle angle measures how the foot rotates in relation to the shank. In our experiment, the subject was equipped with 8 IMU sensors fixed on his body by straps at locations including the back (torso), pelvis, middle of the left and right thighs, middle of the left and right shanks, and the toes. The directions of each IMU are shown in figure 1(a) and (b). The sampling frequency was set to 18 Hz in the experiment.

As a standard, we employed a 17-camera optical motion capture system (Qualisys, Sweden) that operates at a frequency of 100 Hz. The system utilizes 42 markers to the individual, as shown in figure 1(c). Each IMU sensor was equipped with four marks surrounding the subject, while bilateral markers were also placed on the shoulders, knees, Achilles tendons, ankles, and heels of the subject to enable accurate tracking of movements.

B. Experimental process

The individual was required to do two movements throughout the data collecting process: (1) a squat in a regular posture, and (2) a squat in a knee valgus position. With their feet shoulder-width apart, facing forward, and their arms at their sides, the subject started each condition from this calibrated position and held it for 5 seconds.

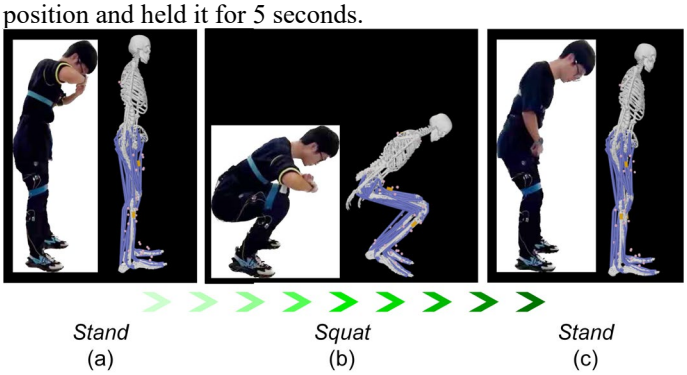

Fig. 2 Data collection and OpenSim analysis process

The image in figure 2 illustrates how the Subject squats. The patient was instructed to squat in each test series until his thighs and shanks formed a roughly 90° angle. Throughout the procedure, the patient was told to maintain a squatting frequency of approximately 0.5 Hz. There were two sets of tests, with 15 squat repetitions in each set. In the initial incident, the patient was standing with his feet shoulder-width apart and his knees pointing about in the same plane as his toes. The second person was standing with his feet shoulder-width apart and his knees valgus-bent.

Then, we used an open source madgwick data fusion technique[13] in MATLAB R2023a to transform the gathered accelerometer, gyroscope, and magnetometer data from each sensor into quaternion data be examined by OpenSim. Next, we computed kinematic estimations based on IMU motion capture using the OpenSim 4.4 [19] program. We employed the Apoorva Rajagopal et al. Full-Body Musculoskeletal Model [20], which has 80 massless muscle-tendon units and 22 stiff joints. The model is appropriate for various motions, including squatting and walking.

In the next step, we used the OpenSense toolkit in OpenSim 4.4 to calculate IMU-based joint kinematics. We imported IMU orientation data generated by the fusion algorithm from the 8 IMU sensors and associated it with the pelvis, according to the

IMU mapping we set up. Then, we performed inverse kinematics (IK) calculations to solve for joint angles q based on Eq. (1).

$$\min_q \sum_{i \in \text{IMUs}} w_i \theta_i^2 \tag{1}$$

where q is the number of IMUs, w_i is the weight of the i-th IMU, and θ_i is the Euler angle measured by the i-th IMU.

After the IK simulation was complete, the collected data could be translated to the musculoskeletal model, as indicated in the in figure 2.

Then, to reduce the influence of modeling and marker data processing mistakes, we carried out residual reduction algorithm (RRA) processing based on the outcomes of IK calculation. We next estimated the CMC (muscle control force). During the simulation, we use the CMC tool to determine the muscle excitation levels that cause the dynamic musculoskeletal model's joint angles to move in the required kinematic direction [19]. The CMC accomplishes this objective by combining static optimization with PD (proportional-differential) control. The computational equation is represented in Eq. (2), as seen in Fig. 3 [21].

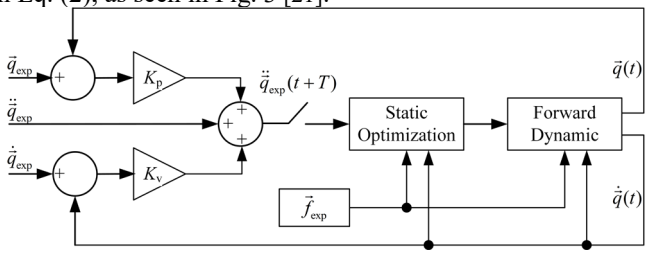

Fig. 3 Schematic of the computed muscle control algorithm [21]

$$\ddot{\vec{q}}^*(t+T) = \ddot{\vec{q}}_{\exp}(t+T) + \vec{k}_v\left[\dot{\vec{q}}_{\exp}(t) - \dot{\vec{q}}(t)\right] + \vec{k}_p\left[\vec{q}_{\exp}(t) - \vec{q}(t)\right]$$

$$J = \sum_{i=1}^{n_x} x_i^2 + \sum_{j=1}^{n_q} w_j \left(\ddot{q}_j^* - \ddot{q}_j\right)^2 \tag{2}$$

$$\begin{cases} J = \sum_{i=1}^{n_x} x_i^2 \\ C_j = \ddot{q}_j^* - \ddot{q}_j \end{cases}$$

where $\ddot{\vec{q}}^*$ which, when achieved, will drive the model coordinates q toward the experimentally derived coordinates $\ddot{\vec{q}}_{\exp}$. $\vec{k}_v$ and $\vec{k}_p$ are the feedback gains on the velocity and position errors, respectively. J is the performance criterion.

To calculate the basic metabolic state of the subject's muscles during the squatting process, we integrated a metabolic calculation probe to the CMC calculation in the Musculoskeletal Model. The calculation's equation is shown as Eq. (3)

$$\begin{cases} P_{\text{met}} = \dfrac{\left(P_{\text{act}} + P_{\text{basal}}\right)}{\eta} \\ P_{\text{act}} = \sum F_{\text{i}} v_{\text{i}} \end{cases} \tag{3}$$

where P_{act} is the mechanical power produced by the muscles and is calculated by adding the power generated by all muscles involved in the movement. P_{basal} is the basal metabolic rate, estimated based on the individual's weight, age, and gender. η is the mechanical efficiency of muscle contraction.

After that, we performed inverse dynamics (ID) calculations to obtain the joint torques during the squatting process.

C. Comparison of IMU and optical motion capture results

In order to evaluate the accuracy of our low-cost IMU motion capture system in capturing deep squatting motion, we compared its results with those of an optical-based motion capture system. The subject performed six sets of deep squat tests while wearing both the marker-based optical system and the IMU device proposed in this study.

Using the optical motion capture data, the model was scaled to calibrate the initial posture, and the marker points were accurately tracked using OpenSim inverse dynamics to determine the motion angles of each joint. These results were then set as a standard reference value for comparison with the measurements obtained from the IMU device.

III. RESULTS AND ANALYSYS

A. Accuracy evaluation for low-cost IMU motion capturing system

During the deep squat tests, the IMU system estimated joint kinematics with a maximum RMSE (root mean square error) of 18.91±1.57° and a minimum RMSE of 4.83±0.64°, as compared to the results obtained from the optical motion capture system. The overall RMSE was 10.10±1.95°. The right hip exhibited a relatively higher degree of inaccuracy in both hip rotation and adduction, indicating that the IMU system tended to overestimate the extent of hip motion changes. However, for all joint angles except for Hip Adduction (L) and Hip Rotation (R), the correlation coefficients between the IMU and optical capture systems were greater than 0.878 (Table II). This suggests that the results obtained from the low-cost IMU motion capture system and the optical system are highly consistent with each other.

TABLE. II RMSE and Correlation Coefficient between low-cost IMU and motion-capture system during deep squatting

Joint	***RMSE(°) Mean ±Std***	***Correlation Coefficient***
Hip Flexion (R)	9.18±1.91	0.985
Hip Flexion (L)	6.17±2.22	0.982
Hip Adduction (R)	18.91±1.57	0.933
Hip Adduction (L)	6.11±0.51	-0.171
Hip Rotation (R)	14.74±2.26	0.767
Hip Rotation (L)	4.83±0.64	0.948
Knee Angle (R)	11.26±2.89	0.982
Knee Angle (L)	10.83±4.64	0.984
Ankle Angle (R)	5.38±1.48	0.943
Ankle Angle (L)	13.61±1.39	0.878

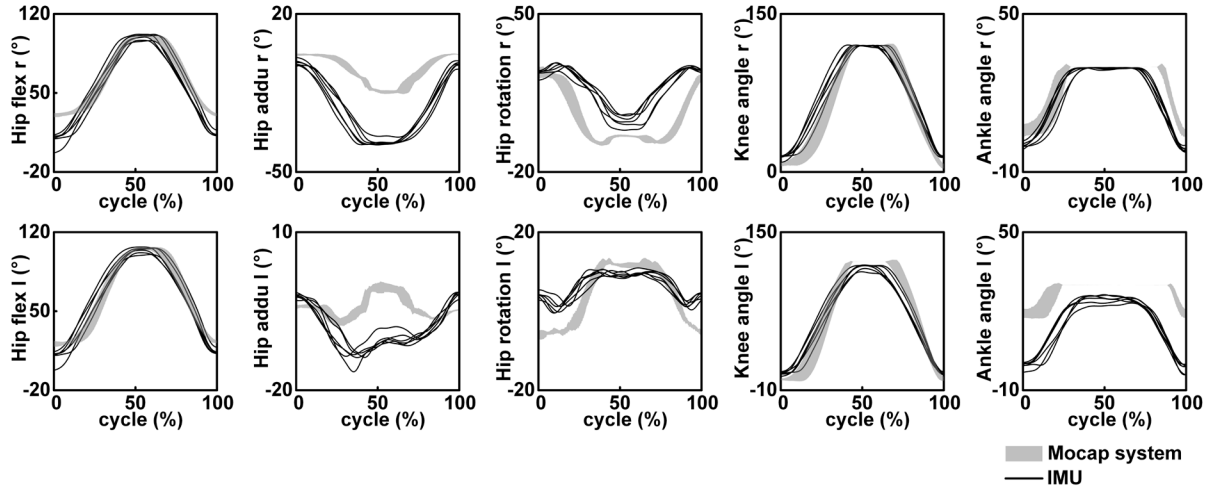

Fig. 4 Joint kinematics acquired by optical capture system and low-cost IMU, respectively.

B. Joint Angle

During the experiment, we analyzed the ankle, knee, and hip angles of each lower limb throughout a squatting cycle, as depicted in figure 5. The results indicated that there were no significant differences in hip adduction, hip rotation, knee angle, and ankle angle between the normal squat and the knee valgus squat. However, compared to the normal squat, the knee valgus squat resulted in an increase of hip flexion in the right and left legs by 18.06% and 13.17%, respectively. This suggests that the primary difference between the two squatting methods is mainly due to the rotation of the hip.

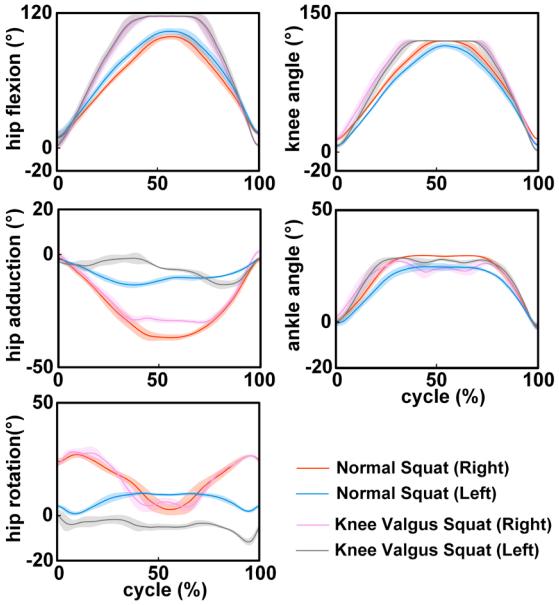

Fig. 5 The joint angles during normal squat and knee valgus squat.

C. Joint Moment

To normalize the results, we divided the joint moment of interest by the subject's weight and obtained the joint moment distribution per unit weight in a single squat cycle, as shown in figure 6.

As illustrated in the figure, the knee valgus squat exhibits a notably consistent torque distribution in hip adduction/rotation as compared to the standard squat, while the directions of hip flexion, knee angle, and ankle angle are slightly altered. Specifically, when the subject squatted to their lowest point, the knee valgus squat resulted in more torque in the direction of hip flexion.

When the subject squatted and stood up during the squat, the knee valgus squat torque exhibited greater fluctuations in the direction of knee angle and ankle angle, with both angles exhibiting higher torque at the lowest point. These findings suggest that an incorrect squatting position could impose greater stress on the ankle, knee, and hip joints, leading to possible joint injury.

From figure 6, it can be seen that the joint torque of the hip is significantly higher than that of other joints during squatting. Therefore, in the design process of an exoskeleton, special attention should be paid to the supporting structure of this joint.

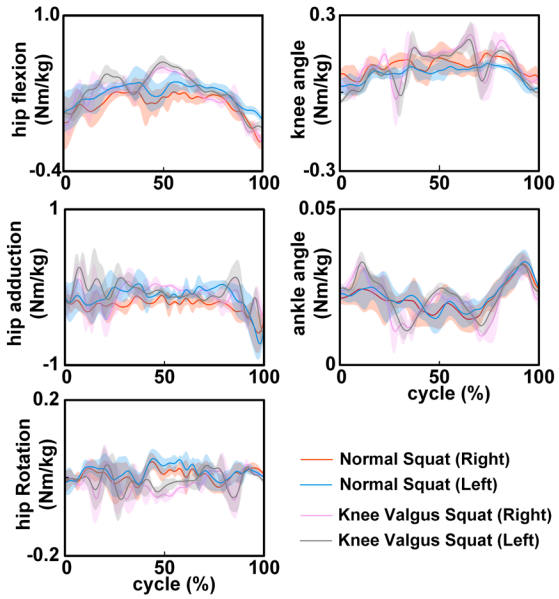

Fig. 6 Joint moments during normal and knee valgus squats.

D. Muscle force

The main muscles that need to be involved in the squat process include biceps femoris long head (bflh), gastrocnemius lateral head (gaslat), gastrocnemius medial head (gasmed), semitendinosus (semiten), sibialis anterior (tibant) and vastus lateralis (vaslat).

Figure 7 depicts the activation levels of the muscles mentioned above, which we determined through Opensim simulation. The results indicate that during knee valgus, the activation of Bflh, Semiten, and Vaslat muscles increased towards the end of the squat. Specifically, the left and right Bflh muscles' activity increased by 54.34% and 35.41%, respectively, while the activation of the left and right Semiten muscles increased by 20.18% and 70.91%, respectively. Both the left and right Vaslats became more activated, by 17.65% and 33.86%, respectively. These findings suggest that an incorrect deep squatting posture requires greater muscular effort to maintain body position during the squat.

In addition, as illustrated in the figure, Tibant was the most activated muscle overall, with its activation level peaking at 1 during both the squat down and stand up phases. Furthermore, its activation duration was longer during knee valgus compared to normal squatting, indicating that this muscle is more susceptible to damage. To mitigate the activation of Tibant and prevent muscular damage, particular attention should be paid to the secondary structure design of Tibant when developing the exoskeleton.

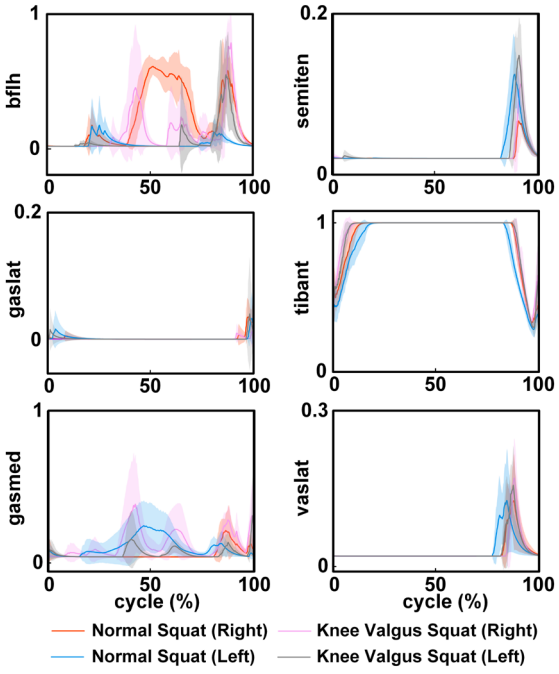

Fig. 7 The muscle forces during normal and knee valgus squatting

We then use the muscle activations to drive our musculoskeletal model using computer muscle control (CMC) method and simulate these two squatting conditions. The total metabolic cost was calculated using a calculator at different time intervals. Figure 8 shows the total metabolic cost ranging from 30 to 80 J. The maximum metabolic cost for normal squatting was 72.97±1.04 J, while that for knee valgus squatting was 74.56±0.97 J. The mean values were similar, but the standard error was more significant for knee valgus squatting, indicating that in some cases, knee valgus squatting may result in higher metabolic cost. In addition, it should be noted that the musculoskeletal model used in this study only includes lower body muscles and cannot represent the overall metabolic cost of the whole body but only reflects the metabolic cost of the relevant muscles during squatting. Future work is required to accurately measure and calculate the metabolic cost of the whole body during squat movement.

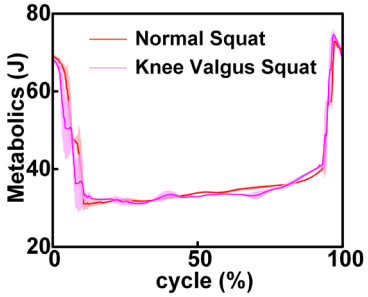

Fig. 8 Metabolism during normal and knee valgus squatting

IV. DISCUSSION

In this paper, we developed a low-cost IMU data-acquisition system for human motion analysis. The system allows researchers to analyze human motion using the OpenSense component in OpenSim software, which can further guide and optimize exoskeleton design based on the analysis results. As demonstration, we conducted two experiments on normal squats and knee valgus squats, respectively. The data collected by the low-cost IMUs were then used in the OpenSim software for inverse kinematics, residual reduction, CMC simulation, and inverse dynamics simulation. We obtained the joint motion angles, torques, and muscle forces in a single squatting cycle. The results confirm that the proposed system is practical, useful, customizable, and affordable for integration in future assistive devices and exoskeletons.

In addition, analysis in figures 3 and 4 reveals that the joint with the highest torque during the squatting process is the pelvis joint, the muscle with the highest activation is the tibialis anterior, and the muscle with the highest force is the soleus, both of which are located in the calf region. Based on these experimental results, we are informed that in the design of exoskeletons, it is necessary to focus on compensating for the torque at the pelvis joint and the muscle force in the calf region during squatting to reduce the likelihood of muscle fatigue-induced injury. In future research, we plan to develop a soft exoskeleton system that is affordable and practical based on these research findings.

V. CONCLUSION

In this research, we have built a low-cost IMU data acquisition system at only ~500 USD, which can be used to capture human squatting movements. The OpenSim software can be used to calculate human motion during the process. We conducted two experiments: normal squats and knee valgus squats, and analyzed joint motion angles, joint torques, muscle forces, and metabolic conditions. The following conclusions can be drawn:

(1) Compared to a normal squat, a knee-out squat increases hip rotation in the right and left legs by 18.06% and 13.17% respectively. This indicates that the differences between the two squatting methods are mainly caused by the rotation of the hip.
(2) Compared with normal squats, knee valgus squats only showed some differences in hip adduction and rotation directions. Incorrect squatting posture may increase the load on the hip joint. In designing exoskeletons, emphasis should be placed on designing the supporting structure of this joint.
(3) During squats, Muscle activation during deep squats with knee valgus shows various levels of increase. And the tibialis anterior muscle has the highest activation level, in designing exoskeletons, emphasis should be placed on designing supporting structures for the Tibialis anterior and soleus muscles to reduce their activation levels and avoid muscle injury.

REFERENCES

[1] H. Grip, K. G. Nilsson, C. K. Häger, R. Lundström, and F. Öhberg, "Does the femoral head size in hip arthroplasty influence lower body movements during squats, gait and stair walking? A clinical pilot study based on wearable motion sensors," *Sensors (Switzerland)*, vol. 19, no. 14, Jul. 2019, doi: 10.3390/s19143240.

[2] J. H. van Dieen, M. J. Hoozemans, and H. M. Toussaint, "Stoop or squat: a review of biomechanical studies on lifting technique," *Clinical biomechanics*, vol. 14, no. 10, pp. 685–696, 1999, [Online]. Available: www.elsevier.com/locate/clinbiomech

[3] M. Kongsgaard *et al.*, "Decline eccentric squats increases patellar tendon loading compared to standard eccentric squats," *Clinical Biomechanics*, vol. 21, no. 7, pp. 748–754, Aug. 2006, doi: 10.1016/j.clinbiomech.2006.03.004.

[4] M. D. Rossi *et al.*, "Use of a squatting movement as a clinical marker of function after total knee arthroplasty," *Am J Phys Med Rehabil*, vol. 92, no. 1, pp. 53–60, Jan. 2013, doi: 10.1097/PHM.0b013e318269d8d0.

[5] D. Panariello, S. Grazioso, T. Caporaso, A. Palomba, G. di Gironimo, and A. Lanzotti, "Evaluation of human joint angles in industrial tasks using OpenSim," in *2019 IEEE International Workshop on Metrology for Industry 4.0 and IoT, MetroInd 4.0 and IoT 2019 - Proceedings*, Institute of Electrical and Electronics Engineers Inc., Jun. 2019, pp. 78–83. doi: 10.1109/METROI4.2019.8792847.

[6] F. Röhrbein *et al.*, "Effect of rearfoot valgus on biomechanics during barbell squatting: A study based on OpenSim musculoskeletal modeling."

[7] X. Li, N. Adrien, J. S. Baker, Q. Mei, and Y. Gu, "Novice Female Exercisers Exhibited Different Biomechanical Loading Profiles during Full-Squat and Half-Squat Practice," 2021, doi: 10.3390/biology.

[8] C. A. Gallo *et al.*, "COMPUTATIONAL MODELING USING OPENSIM TO SIMULATE A SQUAT EXERCISE MOTION." [Online]. Available: www.postersession.com

[9] O. Bordron, C. Huneau, E. le Carpentier, and Y. Aoustin, "Human squat motion: joint torques estimation with a 3D model and a sagittal model", [Online]. Available: https://hal.science/hal-03000335

[10] Y. Lu, Q. Mei, H. te Peng, J. Li, C. Wei, and Y. Gu, "A Comparative Study on Loadings of the Lower Extremity during Deep Squat in Asian and Caucasian Individuals via OpenSim Musculoskeletal Modelling," *Biomed Res Int*, vol. 2020, 2020, doi: 10.1155/2020/7531719.

[11] G. di Raimondo *et al.*, "Towards optimised IMU-based monitoring of joint kinematics and loading in osteoarthritis subjects," *Gait Posture*, vol. 90, pp. 44–45, Oct. 2021, doi: 10.1016/j.gaitpost.2021.09.023.

[12] Z. Sawacha, P. Zancanaro, I. Jonkers, G. di Raimondo, and B. A. Killen, "Comparison of knee loading during walking via musculoskeletal modelling using marker-based and IMU-based approaches SUPERVISOR CANDIDATE."

[13] M. al Borno *et al.*, "OpenSense: An open-source toolbox for inertial-measurement-unit-based measurement of lower extremity kinematics over long durations," *J Neuroeng Rehabil*, vol. 19, no. 1, Dec. 2022, doi: 10.1186/s12984-022-01001-x.

[14] Y. S. Chan, Y. X. Teo, D. Gouwanda, S. G. Nurzaman, A. A. Gopalai, and S. Thannirmalai, "Musculoskeletal modelling and simulation of oil palm fresh fruit bunch harvesting," *Sci Rep*, vol. 12, no. 1, Dec. 2022, doi: 10.1038/s41598-022-12088-6.

[15] M. v. McCabe, D. W. van Citters, and R. M. Chapman, "Developing a method for quantifying hip joint angles and moments during walking using neural networks and wearables," *Comput Methods Biomech Biomed Engin*, vol. 26, no. 1, pp. 1–11, 2023, doi: 10.1080/10255842.2022.2044028.

[16] A. Khandan, R. Fathian, J. P. Carey, and H. Rouhani, "Measurement of temporal and spatial parameters of ice hockey skating using a wearable system," *Sci Rep*, vol. 12, no. 1, Dec. 2022, doi: 10.1038/s41598-022-26777-9.

[17] P. Slade, M. J. Kochenderfer, S. L. Delp, and S. H. Collins, "Sensing leg movement enhances wearable monitoring of energy expenditure," *Nat Commun*, vol. 12, no. 1, Dec. 2021, doi: 10.1038/s41467-021-24173-x.

[18] P. Slade, A. Habib, J. L. Hicks, and S. L. Delp, "An Open-Source and Wearable System for Measuring 3D Human Motion in Real-Time," *IEEE Trans Biomed Eng*, vol. 69, no. 2, pp. 678–688, Feb. 2022, doi: 10.1109/TBME.2021.3103201.

[19] S. L. Delp *et al.*, "OpenSim: Open-source software to create and analyze dynamic simulations of movement," *IEEE Trans Biomed Eng*, vol. 54, no. 11, pp. 1940–1950, Nov. 2007, doi: 10.1109/TBME.2007.901024.

[20] A. Rajagopal, C. L. Dembia, M. S. DeMers, D. D. Delp, J. L. Hicks, and S. L. Delp, "Full-Body Musculoskeletal Model for Muscle-Driven Simulation of Human Gait," *IEEE Trans Biomed Eng*, vol. 63, no. 10, pp. 2068–2079, Oct. 2016, doi: 10.1109/TBME.2016.2586891.

[21] D. G. Thelen and F. C. Anderson, "Using computed muscle control to generate forward dynamic simulations of human walking from experimental data," *J Biomech*, vol. 39, no. 6, pp. 1107–1115, 2006, doi: 10.1016/j.jbiomech.2005.02.010.